ELSEVIER

Chemistry and Physics of Lipids
77 (1995) 13–23

Chemistry and Physics of LIPIDS

Formation of gel and fibrous microstructures by 1-alkyne amphiphiles bearing L-serine headgroup in organic solvents

Kaliappa G. Ragunathan, Santanu Bhattacharya*

Department of Organic Chemistry, Indian Institute of Science, Bangalore 560012, India

Received 21 December 1994; revision received 29 March 1995; accepted 5 April 1995

Abstract

The study of amphiphiles that form non-spheroidal, and other assemblies, upon solvation is the key to understanding the relationship between molecular structure and supramolecular morphology. With this aim in mind, we have employed L-serine and L-histidine derivatives that are linked via amide bond to hydrophobic chain. L-Serine amphiphiles form gels in $CHCl_3$, CH_2Cl_2 and CCl_4. Microscopic examinations of these gels reveal the coexistence of tubules, helical ribbons, and spheres. On the other hand, they produce only spherical structures and rods when dispersed in aqueous media (phosphate buffer). In contrast, amphiphiles based on the L-histidine group, neither formed any gel nor produced any microstructures in non-aqueous solvents like $CHCl_3$, but produced spherical structures and helical rods in water. We also examined the effect of introducing 1-yne or 1-ene moieties into the hydrocarbon chain of such amphiphiles. These moieties, when present in the hydrophobic segment, do not perturb the supramolecular assembly features of the respective serine amphiphiles. Actually, 1-yne moiety, when present in the hydrophobic portion of the amphiphiles, gives characteristic UV-fine structures upon aggregation in water and might be used as a non-invasive marker for probing critical aggregate concentration.

Keywords: Serine amphiphiles; Histidine amphiphiles; 1-yne moiety; Chloroform gel; Helical ribbons; Tubules; Multilamellar spherical structures

1. Introduction

Supramolecular assemblies composed of chiral amphiphiles produce diverse microstructures such as tubules, cylinders, helical rods, liposomes, etc. For example, tubular microstructures were observed with L-glutamate-attached amphiphiles, [1] poly(L-aspartic acid) derivatives, [2] and diacetylenic phosphocholine lipids [3–5]. Other amphiphiles, such as bile salts [6], hydroxy and non-hydroxy fatty acid cerebrosides [7,8] and galactosylceramide [9] form cylinders or tubules. In contrast, *N*-acyl-L-aspartic acids and *N*-acyl-β-alanine gave only fibrous cylindrical aggregates [10]. Helical bilayer organization was earlier reported from nucleoside-attached phospholipids

* Corresponding author, Fax: 91-80-3341683; E.Mail address: ochsb@orgchem.iisc.ernet.in.

SSDI 0009-3084(95)02450-W

[11] and from unpolymerized and polymerized diacetylene aldonamides [12]. All of these microstructures were observed in aqueous dispersions. Recently, Fuhrhop et al. [13] have shown that naturally occurring chiral hydroxy amphiphile in organic solvents, like $CHCl_3$, form tubular structures. Nevertheless, an account of microstructure formation of amino acid-bearing amphiphiles in non-aqueous media is still lacking in the literature.

In this work, we have examined the supramolecular association behaviour of L-serine and L-histidine based amphiphiles having 1-alkyne moiety (in the hydrophobic chain) in non-aqueous solvents, i.e. $CHCl_3$, CCl_4, CH_2Cl_2, and also in water. The 1-yne moiety has been introduced to explore the influence of this moiety on the aggregation behaviour of the amphiphiles, since 1-ynes are also capable of associating through hydrogen bonding [14]. In addition, 1-ynes are precursors to diyne lipids which form nanostructures [15]. High degrees of freedom are associated with terminal methyl groups of the fatty acid chains in membranes relative to that, e.g. methylene groups, in the middle of the chain [16]. We thought that if introduced, terminal 1-ynes might mitigate the chain mobility. If desired, the tails may also be knotted by polymerizing the 1-yne unit through X-ray irradiation [17]. In order to elucidate the role (if any) of 1-yne moieties upon aggregation towards microstructure formation under the same experimental conditions, we have also prepared L-serine amphiphiles that have an alkanoyl or an 1-alkenoyl chain.

We report, herein, the synthesis of these amphiphiles (**4a–c**, **6**) and the results of their aggregation behaviour in water and in non-aqueous solvents, e.g. chloroform. The microstructure-forming abilities of different aggregates have also been examined in detail. Finally, based on these experimental findings, we provide a rationale for such assembly behaviour with the help of molecular modelling studies.

2. Materials

Undecylenic acid, 1,3-dicyclohexylcarbodiimide (DCC), L-serine, L-histidine, phosphotungstic acid and calcium hydride were from Aldrich Chemical Co. (Milwaukee, WI). Thionyl chloride, triethylamine, sodium hydroxide, sodium sulfate, magnesium, disodium hydrogenphosphate, sodium dihydrogenphosphate dihydrate, sulfuric acid and hydrochloric acid were from SD-Fine Chemicals (Bombay, India). All solvents used were of highest grade commercially available and purified, dried or freshly distilled before use: CCl_4, $CHCl_3$ and CH_2Cl_2 from P_2O_5, Et_3N from CaH_2, MeOH from activated Mg-turnings. A 1 M, pH 7.8, phosphate buffer was prepared by mixing solutions of Na_2HPO_4 and $NaH_2PO_4 \cdot 2H_2O$.

3. Methods

3.1. General procedure

Fourier transform ^{1}H-NMR spectra were recorded on either a Bruker SEM 200 (200 MHz) or Jeol FX 90 (90 MHz) instrument. Chemical shifts (δ) are reported in ppm downfield from the internal standard. IR spectra were recorded with Perkin-Elmer 781 instrument either in Nujol or as neat sample using polystyrene as standard and are reported in wavenumbers (cm^{-1}). The UV-visible spectra were recorded in a Shimadzu Model 2100

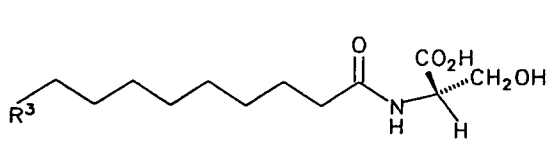

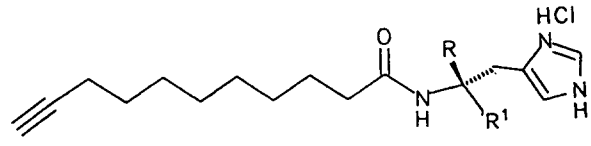

4a, R^3 = C≡CH, 4b, R^3 = CH=CH$_2$, 4c, R^3 = CH$_2$CH$_3$ 6, R = CO$_2$H, R^1 = H

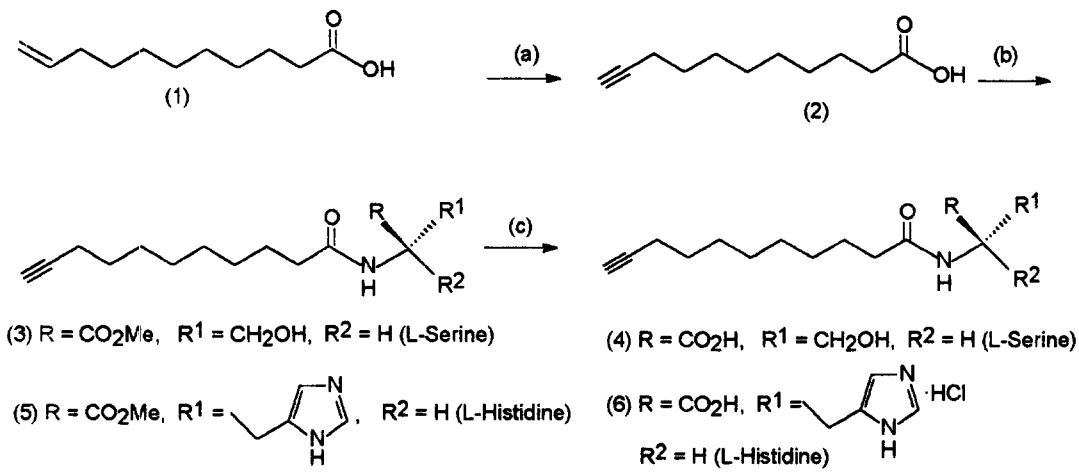

Scheme 1. (a) (i) Br_2-$CHCl_3$ (ii) KOH-H_2O, Reflux, H_3O^+, 42%; (b) DCC, Et_3N, $CHCl_3$, MeO_2C—$CH(R^1)NH_2$·HCl, RT, ($R^1 = CH_2OH$, 64%; $R^1 = CH_2Im$·2HCl, 59%); (c) NaOH (0.5 M), RT, CH_3OH—H_2O, HCl, pH 3, ($R^1 = CH_2OH$, 94%; $R^1 = CH_2Im$·HCl, 85%).

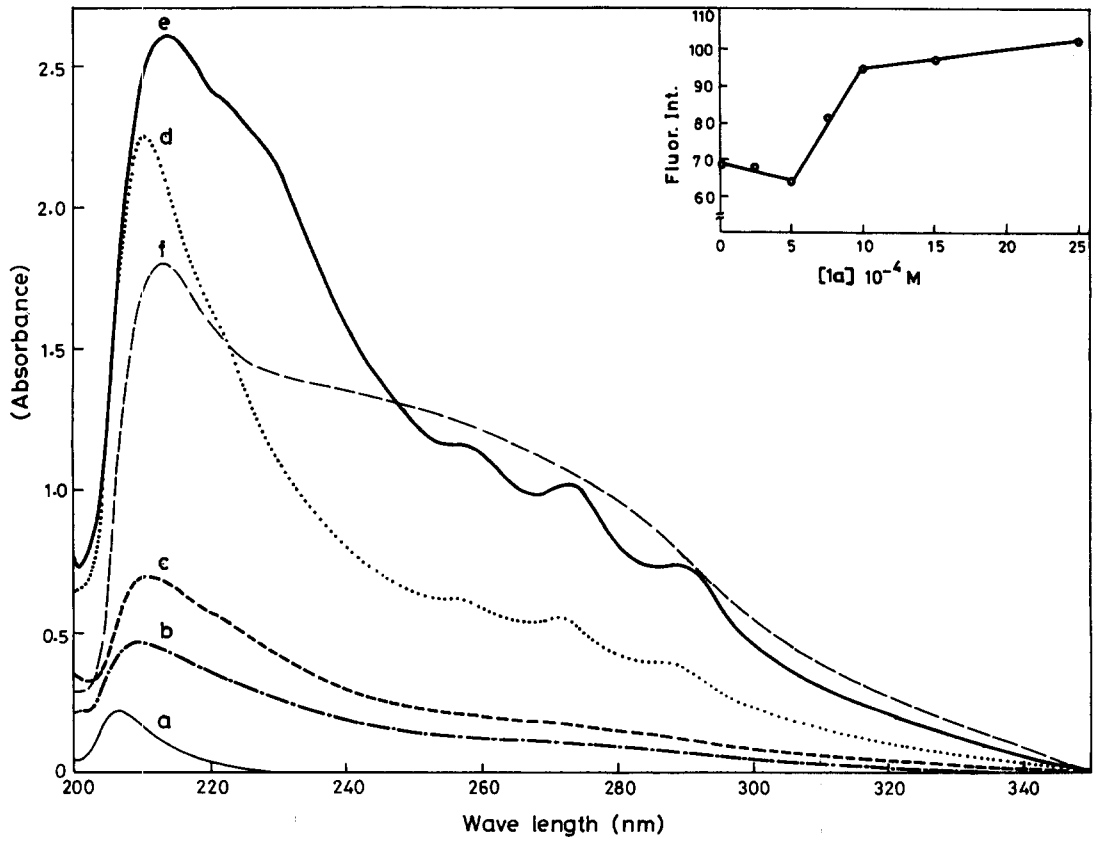

Fig. 1. UV-vis absorption spectra of **4a** in aqueous buffer (pH 7.8) at various concentrations. (a) 0.1 mmol, (b) 0.25 mmol, (c) 0.5 mmol, (d) 1 mmol, (e) 20 mmol, (f) 100 mmol. Inset: plot of fluorescence intensity (doped DPH) vs. concentration of amphiphile **4a**.

UV-visible spectrophotometer. Elemental analyses were performed on a Carlo Erba elemental analyzer Model 1106 and are reported as percentages. Analytical TLC were performed with 0.25 mm thick precoated silica gel glass plates 60F-254 (Merck). The melting points were determined on a unimelt melting point apparatus in open capillaries and were uncorrected.

3.2. Measurement of critical micellar concentration

Different aqueous solutions containing 2 μmol of DPH (1,6-diphenyl hexatriene) having different concentrations (100–0.01 mmol) of the amphiphiles were prepared. The steady-state fluorescence measurements were carried out using Shimadzu RF-540 spectrofluorimeter with quartz cuvettes of 1 cm pathlength. The excitation wavelength was 358 nm and the emission wavelength was 430 nm. Onset of micellar assembly at a particular amphiphile concentration was indicated by the sudden increase in the fluorescence intensity of the doped DPH.

3.3. Electron microscopy

The supramolecular assemblies of amphiphiles in aqueous solution were examined by JEOL 840A scanning electron microscope. The respective aqueous dispersions were spread on iron troughs and coated with gold. The gold-coated samples were observed under the microscope with magnifications of 1400 ×, 1000 ×, 500 × and 450 ×.

3.4. Optical microscopy

The supramolecular aggregates in organic solvents were examined using a Bright-field optical microscope Neophot-21 connected to a SLR camera. The sample dispersions were spread out on freshly cleaned glass slides and kept in the dark for 24 h and were observed at magnifications of 100 ×, 400 × and 500 ×.

3.5. Circular dichroism

CD spectra were recorded at 25°C with a Jasco J-500A spectropolarimeter using a DP-500N data processor with cells of 2 mm pathlength equipped with thermostatted water-circulating bath. Most samples were examined at ~1 mmol concentration. Each CD spectral scanning was repeated three times to ensure reproducibility and, in all cases, spectral recordings were repeated with different sample preparations of a given amphiphile.

3.6. Molecular modelling

Computations of optimized structures were carried out with Insight II 2.3.0 (Biosym Tech.) software using Discover forcefield and steepest descent algorithm.

3.7. Synthetic methods

3.7.1. 10-Undecynoic acid (2)

10-Undecynoic acid (**2**) was prepared from 10-undecenoic acid (**1**) by minor modification of the literature procedure [18] as described in the following. 10-Undecenoic acid was converted to 10,11-dibromoundecanoic acid in quantitative yield by bromination with Br_2 in $CHCl_3$. This was dehydrobrominated to 10-undecynoic acid by refluxing with aqueous KOH (0.1 M) for 8 h. The solution was cooled overnight and brought to pH 4 by adding 2N H_2SO_4 and the floating oily layer was extracted with $CHCl_3$. The $CHCl_3$ layer was dried over anhyd. Na_2SO_4, the solvent was evaporated and the residue was distilled under reduced pressure (6 mm), when the 10-undecynoic acid was collected at 140–160°C (42%), mp. 41°C, lit. mp. 41–42°C [19].

3.7.2. N-10-Undecynoyl-L-serine methyl ester (3)

The L-serine methyl ester hydrochloride (L-Ser.OMe.HCl) was prepared by the following procedure. To an ice-cold dry methanol (30 cm^3), 2 cm^3 of $SOCl_2$ was slowly added with stirring. To this solution, L-serine (2 g, 1.8 mmol) was added and stirred at ambient temperature for 24 h. Then, the solution was concentrated, and to it, Et_2O was added to induce precipitation of L-serine methyl ester hydrochloride. The colorless solid thus precipitated was filtered off, washed with ether and dried in a vaccum desiccator (2.8 g, 97%); mp. 156–157°C; IR, ν_{max}(Nujol, cm^{-1}) 1735 [—C=O, ester], 3300 (—OH).

To a solution of freshly distilled anhyd. Et_3N (200 mg, 2 mmol) in dry $CHCl_3$ (10 cm^3), L-

Ser.OMe.HCl (155 mg, 1 mmol) was added and stirred. To this, a solution of undecynoic acid (**2**) (182 mg, 1 mmol) and DCC (210 mg, 1 mmol) in dry $CHCl_3$ (30 cm^3) were added dropwise. After the addition was over, the reaction mixture was stirred at ambient temperature for 24 h. The solid DCU was separated by filtration and the filtrate, on solvent evaporation, gave a thick oil, which was purified by column chromatography over silica gel (230–400 mesh) [$CHCl_3$-MeOH (96:4)], (154 mg, 64%); IR, ν_{max} (Neat/cm^{-1}) 1530 (amide-II), 1640 (amide-I), 1735 (—C=O, ester), 2100 (C≡C), 3320 (acetylene C—H) and 3360 (amide N—H); ^{1}H-NMR (90 MHz; $CDCl_3$), δ_{ppm}, 1.36 (12H, br s, —CO—CH_2—(CH_2)$_6$—CH_2—), 2.3 (5H, m, —CO—CH_2—, —C≡C*H* and —C≡C—CH_2—), 3.80 (3H, s, —OCH_3), 3.96 (2H, d, —CH_2OH) and 4.70 (m, 1H, chiral—C*H*).

*3.7.3. N-Undecynoyl-L-serine (**4a**)*

The compound **3** (142 mg, 0.5 mmol) was stirred in (1:1) aqueous methanolic 0.5 N NaOH solution for 24 h. Then, the solution was acidified with 2N HCl and the pH was brought to 4. The aqueous layer was extracted with $CHCl_3$ (3 × 25 cm^3) and the $CHCl_3$ layer was dried over anhyd. Na_2SO_4. The removal of solvent from this solution gave a gel which became solid on drying in vaccum (126 mg, 94%), mp. 72°C. Analysis (Found: C, 56.12; H, 8.44; N, 4.54. $C_{14}H_{23}NO_4 \cdot 1.75H_2O$ requires C, 55.89; H, 8.87; N, 4.65). IR, ν_{max} ($CHCl_3$/cm^{-1}); 1540 (amide-I), 1610 (amide-II), 1734 (—C=O, acid), 2100 (C≡C), and 3328 (acetylenic—CH). ^{1}H-NMR (200 MHz; $CDCl_3$), δ_{ppm} 1.35 (10H, br s, —CO—CH_2—CH_2—(CH_2)$_5$—CH_2—), 1.65 (2H, t, —CO—CH_2—CH_2—), 2.08 (1H, t, —C≡C*H*), 2.17 (2H, t, HC≡C—CH_2—), 2.32 (2H, t, —CO—CH_2—), 3.9 (2H, m, —CH_2OH) and 4.57 (1 H, quintet, chiral C*H*). The amphiphiles **4b** and **4c** were prepared from 10-undecenoic acid or *n*-undecanoic acid and L-serine methyl ester by following a similar procedure as that described for **4a**. Relevant details for their characterization are given below. **4b**: analysis (Found: C, 59.04; H, 9.59; N, 4.76. $C_{14}H_{25}NO_4$ requires C, 59.03; H, 9.38; N, 4.92). ^{1}H-NMR (200 MHz; $CDCl_3$), δ_{ppm}, 1.30 (10H, br s, —CO—CH_2—CH_2—(CH_2)$_5$—CH_2—), 1.65 (2H, t, —CO—CH_2—CH_2—), 2.02 (2H, m, —CH_2—CH=CH_2), 2.32 (2H, t, —CO—CH_2—), 3.98 (2H, m, —CH_2OH), 4.65 (1H, quintet, chiral—C*H*), 4.95 (2H, m, —CH=CH_2), 5.89 (1H, m, —C*H*=CH_2), 6.9 (1H, br s, —CO—N*H*). **4c**, analysis (Found: C, 57.40; H, 10.23; N, 4.95. $C_{14}H_{27}NO_4 \cdot H_2O$ requires C, 57.71; H, 10.03; N, 4.81). ^{1}H-NMR (200MHz; $CDCl_3$ and acetone-d_6), δ_{ppm}, 0.83 (3H, t,—CH_3), 1.30 (14H, br s, —CO—CH_2—CH_2—(CH_2)$_7$—CH_2—), 1.65 (2H, t, —CO—CH_2—CH_2—), 2.33 (2H, t, —CO—CH_2—), 3.9 (2H, m, —CH_2—OH), 4.6 (1 H, quintet, chiral—C*H*).

*3.7.4. N-Undecynoyl-L-histidine methyl ester (**5**)*

To an ice-cold methanol (100 cm^3), $SOCl_2$ (2 cm^3) was added slowly and to this solution L-histidine (3.1 g) was added and stirred at ambient temperature for 48 h. Then, methanol was completely removed by evaporation and the solid obtained was washed with ethyl ether and air dried (4 g; 82%); mp. 198°C.

To a suspension of L-histidine methyl ester dihydrochloride (242 mg, 1 mmol) in $CHCl_3$ (40 cm^3) Et_3N (300 mg, 3 mmol) was added and stirred. To this undecynoic acid **2** (182 mg, 1 mmol) and DCC (210 mg, 1 mmol) in $CHCl_3$ (25 cm^3) was added and stirred for 24 h. The floating DCU was filtered off. The filtrate, on evaporation of solvent, gave a gummy mass which was purified by silica gel column chromatography [$CHCl_3$-MeOH (92:8)] (197 mg, 59%). IR, ν_{max} ($CHCl_3$/cm^{-1}), 1540 (amide-I), 1630 (amide-II), 1735 (—C=O, ester), 2100 (C≡C) and 3280 (acetylenic —CH). ^{1}H-NMR (90 MHz; $CDCl_3$), δ_{ppm}, 1.36 (12H, br s, —C≡C—CH_2—(CH_2)$_6$—), 2.24 (5H, m, *H*C≡C—CH_2— and —CH_2—CO—), 3.16 (2H, d, —CH_2—Im), 3.76 (3H, s, OCH_3), 4.9 (1H, m, chiral—C*H*), 6.84 and 7.64 (2H, s, 2 imidazole *H*s).

*3.7.5. N-Undecynoyl-L-histidine (**6**)*

The ester **5** (334 mg, 1 mmol) was stirred with 0.5N NaOH in methanol/water (1:1 v/v) for 10 h. Then, the solution was acidified with 2N HCl and the pH adjusted to 3. The aqueous layer was extracted with $CHCl_3$/MeOH (1:1 v/v), several

solvents and drying in vacuum, gave an oily substance (302 mg; 85%). IR ν_{max} (Nujol/cm^{-1}), 1540 (amide-I), 1610 (amide-II), 1700 (—C=O acid), 2100 (C—C), and 3280 (acetylenic—CH). Analysis (Found C, 54.16; H, 7.74; N, 11.53. $C_{17}H_{26}ClN_3O_3 \cdot 1.25H_2O$ requires C, 53.96; H, 7.60; N, 11.10). ^{1}H-NMR (90 MHz; D_2O), δ_{ppm}, 1.1–1.8 (12H, br s, —CO—$CH_2(CH_2)_6$—), 2.15 (5H, m, $HC{\equiv}C$—C—CH_2— and —CH_2—CO), 3.25 (2H, m, —CH_2Im·HCl), 4.9 (1H; m, chiral—C*H*) and 7.3 and 7.6 (2H, s, 2 imidazolium *H*s).

4. Results and discussion

4.1. UV-vis spectral studies of aqueous dispersions

The concentration dependent UV-visible studies of the amphiphiles **4a**–**4c** in phosphate buffer, pH 7.8 and **6** in water showed interesting spectral features. Fig. 1 shows the UV-visible spectrum of different concentrations of **4a**. At a concentration of 0.5 mmol, it showed an amide absorption at ~205 nm and an acetylenic absorption at 267 nm. At a concentration above 0.5 mmol, a remarkable spectral change was observed. The fine-structures at 255, 272 and 288 nm due to the 1-yne moiety with concomitant red-shift of the amide absorption to 213 nm were seen. The changes in the UV-visible signatures presumably indicate micelle formation which was independently checked by fluorescence spectroscopy (see below). The red-shift in the amide absorption upon an increase in concentration is suggestive of hydrogen-bonding interaction [20] among amide groups in the supramolecular aggregate. Above 20 mmol of **4a**, only broadened spectrum, with a further decrease in absorption intensity, was obtained. This probably indicates the onset of further aggregation [21] of the amphiphiles beyond regular micelle formation, presumably, due to generation of non-spheroidal shapes at >20 mmol concentration (see below). Other examples are known, where the morphology of the aggregate changes when the amphiphile concentration markedly exceeds the critical micellar concentration (cmc) [22]. The post-micellar [22] association is presumably assisted by monomer-monomer hydrogen-bonding contacts [20] at the level of amphiphile headgroups.

The amphiphile **6** when dispersed in pH 7.8 phosphate buffer aqueous media also showed the acetylene fine-structures at 248, 256 and 262 nm, above the concentration of 1 mmol. Below this concentration a single band due to 1-ynes at 255 nm was obtained. The fine-structures due to acetylene moieties in **6** are blue-shifted and closely spaced when compared with that of **4a**. However, in this case the amide absorption could not be clearly detected due to the overlapping imidazolium absorption.

The L-serine amphiphiles **4a**–**4c** dispersed well in phosphate buffer (pH 7.8) and when gently shaken, formed micellar aggregates. The onset of micellization for dispersions of **4a**, **4b**, **4c** were also examined by measuring the steady-state fluorescence intensities of DPH as a function of amphiphile concentration. This methodology, based on fluorescence spectroscopy, has been exploited by others [23] to estimate the cmc. A representative example of the cmc determination by this method for **4a** is given in Fig. 1 (inset). The cmc for **4a** was found to be ~0.8 mmol. The corresponding value for **4b** was 0.7 mmol. However, the cmc for **4c** was considerably lower (~0.3 mmol). The L-histidine amphiphile **6** also readily dissolved in water and formed micellar aggregates. The cmc value for **6** in water was found to be ~1.2 mmol by this method.

It is clear that the fine-structures of acetylene moieties of **4a** and **6** appear above their cmc value. These fine-structures might originate from mutual 'through space interaction' [24] between acetylene moieties in the supramolecular assembly of the 1-yne amphiphiles. Thus, the acetylene moiety might be considered as a non-invasive probe to estimate critical aggregation phenomena.

4.2. Supramolecular assembly in chloroform and the formation of gel

The UV-visible spectrum of **4a** in $CHCl_3$ at 0.2 mmol showed the acetylene fine-structures at 259, 274 and 291 nm and the amide band at 240 nm indicating the aggregation of **4a** even at this low concentration. This suggests that hydrogen-bonded association among amide groups is

stronger in $CHCl_3$ than that in basic aqueous medium where the amide absorption occurs at 213 nm. In aqueous solution (pH 7.8), the hydrogen-bonding network is weakened probably due to, (a) the ionization of—CO_2H, leading to the formation of—CO_2^- anions and this would lead to net repulsion at the level of headgroups; (b) the presence of water molecules at the micellar interface which might compete for hydrogen-bonding.

The L-serine amphiphiles **4a**, **4b**, **4c** when dissolved, above 6 mmol concentration, in either of the solvents $CHCl_3$, CH_2Cl_2 or CCl_4 at room temperature, produced 'firm solid gels'. Histidine amphiphile **6** did not dissolve in $CHCl_3$. It dissolved in $CHCl_3$ only in presence of 1 equiv. of Et_3N, but the resulting mixture did not form a gel.

4.3. Microstructure formation from gel

The gels, thus generated at >6 mmol concentration, melted into liquid upon heating to 45°C or above. The liquified material from $CHCl_3$ gel of **4a** showed three interesting microstructures when examined under bright-field optical microscope. This consisted of, (a) giant [25] multilamellar spherical structures (Fig. 2a), (b) tubules (Fig. 2b), and (c) right-handed helical ribbons of width 15–30 μM (Fig. 2c). Very long tubules, up to 3000 μM in length with a diameter of 5–20 μM, were also seen (Fig. 2b). Giant spherical structures from amino acid-derived amphiphiles are not unprecedented [25]. The microstructures obtained for samples dispersed in non-aqueous solvent might not represent the same aggregates present as micellar solutions. This is also indicated from the dimension of the observed structures. The number of spherical structures, however, progressively decreased with time at the expense of their conversion into helical ribbons or to tubules. Kunitake et al. [1] also observed similar type of transition in double-chain glutamate lipids in aqueous media. Yager et al. [3] observed the conversion of vesicles to tubules of high length-to-width ratio, when double-chain diyne lipid was cooled through its phase transition temperature. It is interesting to note, however, that even with singe-chain amphiphiles in non-aqueous media, similar morphological transition could be possible, as evident in the present case. The intertwining and entangling of the long tubules in the serine amphiphile, like the polymer coils in the polyacrylamide and polystyrene gels [26] and hydrogen-bonding interactions through secondary amide chains, could be the plausible reasons for the formation of the gel. In fact, subtle change in the solvent environment such as addition of petroleum ether to a 2mmol solution of **4a** in $CHCl_3$, induces precipitation of intertwined and entangled tubules as observed under the optical microscope (Fig. 2d). The gels produced in CH_2Cl_2 and CCl_4 also showed similar microstructures as that of the $CHCl_3$ gels. This suggests that the microorganizations of the amphiphilic assemblies are probably similar in these organogels.

Recently, the mechanism of formation of tubules from vesicles through helical ribbons was examined by Schnur et al. [27]. In the light of this scheme, we suggest that large multilamellar vesicles from chiral amphiphiles first develop stripes in the molecular orientation, separated by sharp domain walls. The lipid aggregates thus formed break-up along these domain walls to form ribbons. The ribbon like sub-assemblies then undergo twist to form helix and the helical structures, presumably, undergo fusion into cylindrical tubules. Whatever may be the actual mechanism, the observation of multilamellar vesicle and related spherical structures and their conversion to helical ribbons and tubules are supportive of the above-mentioned scheme of tubule formation and, indeed, provide experimental evidence for this scheme [27]. One can also find similar transformation of spherical multilamellar vesicles into tubules from other systems, although the latter ones are not at all related in terms of molecular structure to L-serine-derived amphiphiles [28]. It is interesting to note that the amphiphiles **4b** and **4c** also produce similar microstructures.

4.4. Microstructures from aqueous dispersions

The SEM examination of the aqueous dispersions of the L-serine and L-histidine amphiphiles also revealed the presence of different organized structures. Thus, 1 mmol of **4a** in phosphate buffer (pH 7.8), produced giant [25] spherical

structures of 10–20 μM in diameter (Fig 2e) and fibrous rods ~ 5 μM in diameter and ~ 50 μM (Fig. 2f). Similar kinds of supramolecular assemblies were observed from the aqueous solution of (phosphate buffer, pH 7.8) **4b** and **4c**. The dispersion of L-histidine amphiphile in water produced two kinds of microstructures. Thus, 1 and 5 mmol of **6** in water produced spherical structures 10–30 μM in diameter (Fig 2g) and rods >200 μM in length(Fig. 2h), respectively.

4.5. Infrared spectral studies

The infrared spectra of **4a**–**4c** in $CHCl_3$ showed the presence of amide-I band at 1610 cm^{-1} indicating hydrogen-bonded amide groups [20] and a band at 1735 cm^{-1}, which could be due to either non-hydrogen bonded or weakly hydrogen-bonded acid carbonyl absorptions [29]. Similar association through hydrogen-bonding among amide groups has also been observed with sphingolipids [21]. On the other hand, histidine amphiphile, **6** in $CHCl_3$ in the presence of 1 equiv. of Et_3N, showed amide-I absorption at 1610 cm^{-1} indicating hydrogen-bonded amide groups and a broad band in the region 1700 cm^{-1} due to non-hydrogen-bonded acid carbonyl groups [29].

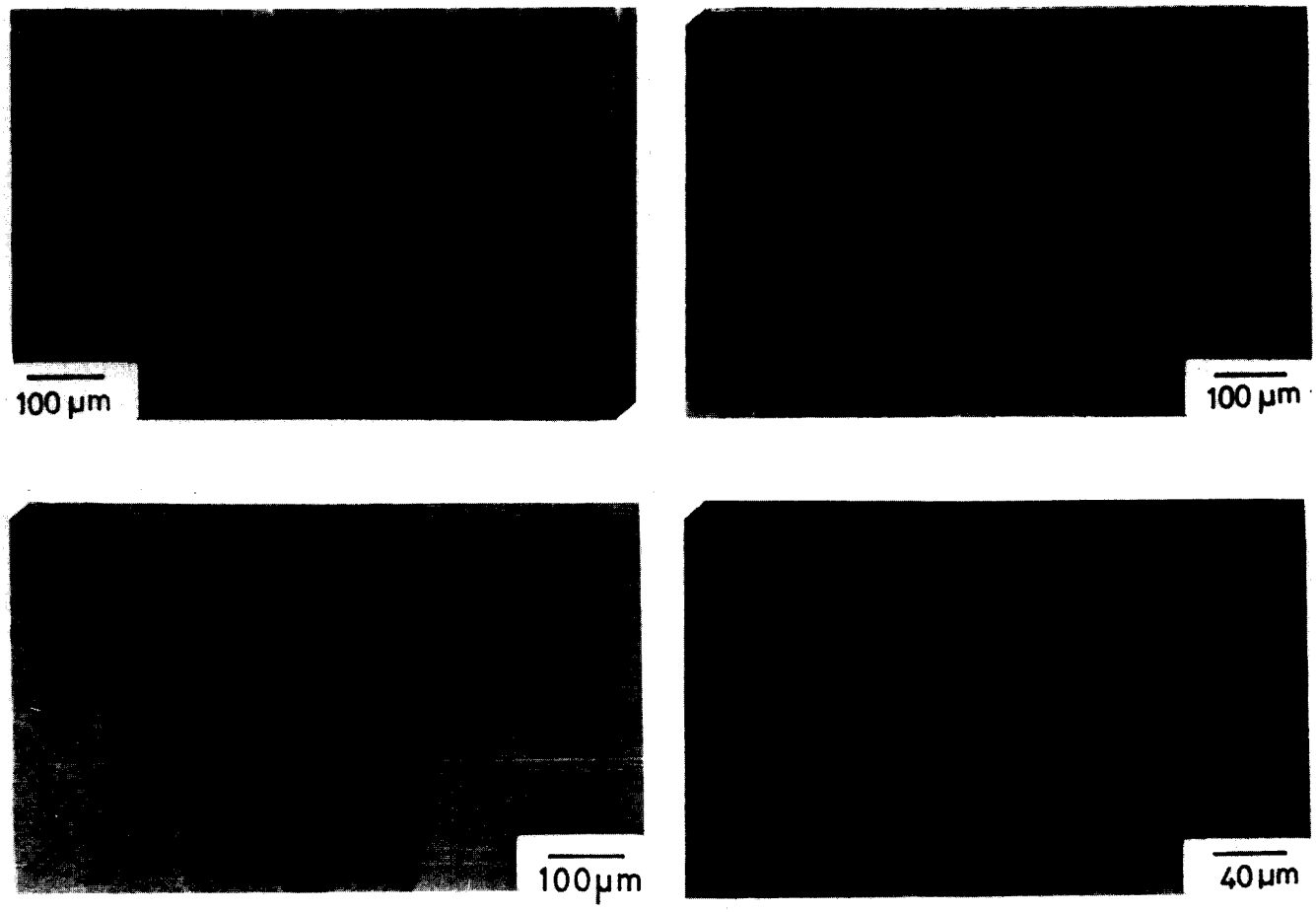

(a)–(d)

Fig. 2. Bright-field optical micrographs. (a) Spherical structures and intertwined tubules, (b) tubules, (c) helical ribbon obtained from 2 mmol **4a** in $CHCl_3$, (d) precipitated tubules of 1 mmol **4a** from chloroform gel by adding petroleum ether. Scanning electron micrographs. (e) Spheres from 1 mmol **4a** in aqueous solution (phosphate buffer, pH 7.8), (f) fibrous rods obtained from aqueous dispersions of 1 mmol **4a** (phosphate buffer, pH 7.8), (g) spherical structures from 1 mmol **6** in water, and (h) helical rods from 5 mmol **6** in water.

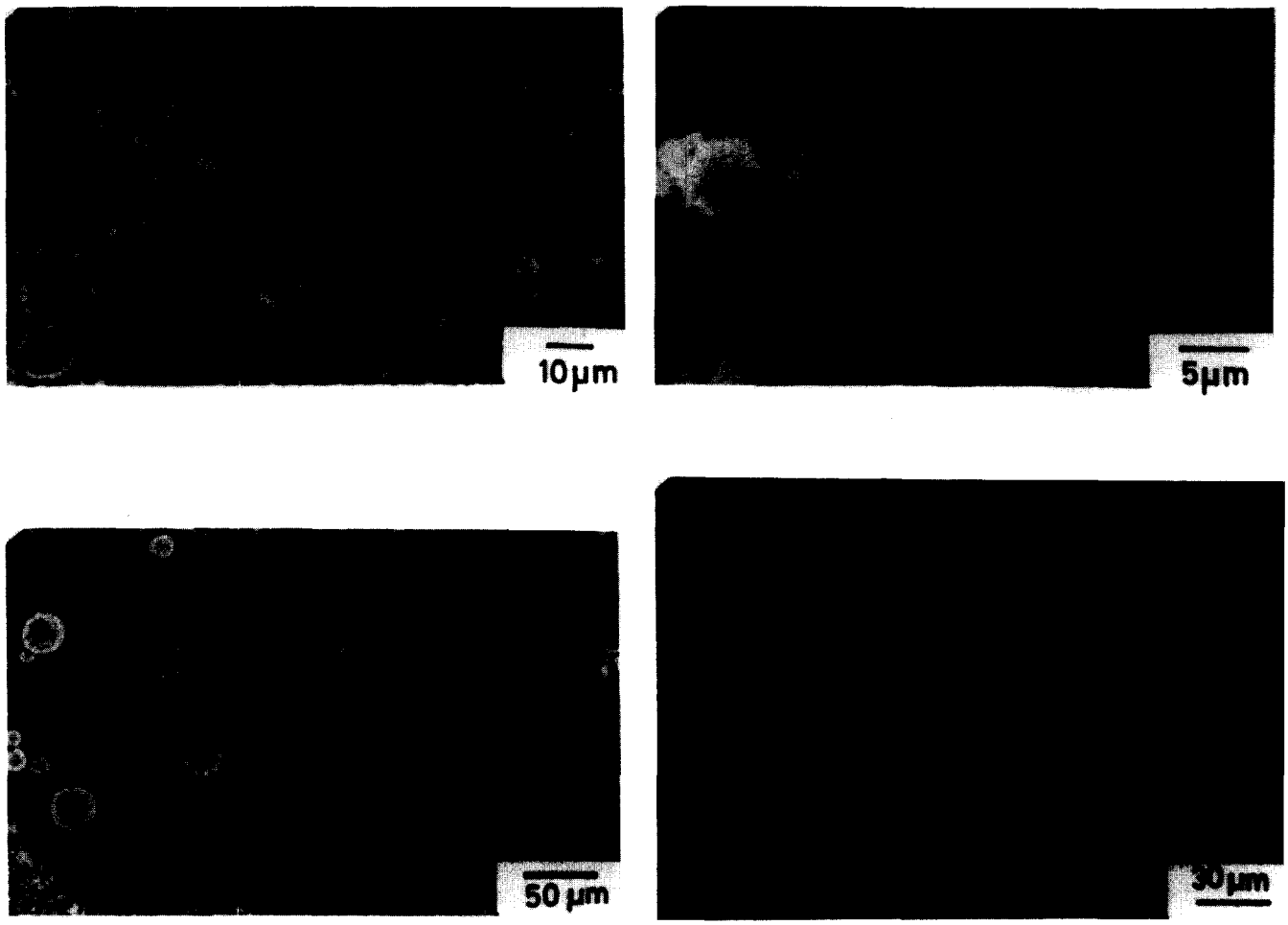

Fig. 2. (e)–(h).

4.6. Circular dichroism studies of aggregates

The CD spectrum of 1 mmol **4a** in phosphate buffer (pH 7.8, and 25°C) gave $[\theta]_{212} = -1.1 \times 10^6$. Concentration-dependent (0.1–10 mmol) CD study of **4a** (phosphate buffer, pH 7.8) showed (data not shown) a red-shift in the spectral band with an increase in concentration of **4a** (i.e. 206 nm to 213 nm). Similar CD spectra were obtained from 1 mmol, **4b** and **4c** ($[\theta]_{212} = -1.4 \times 10^6$ and -1.15×10^6, respectively). In contrast, 1 mmol **6** in water gave $[\theta]_{214} = +2 \times 10^7$. However, as in the case of **4a**–**4c**, the spectral band position of **6** red-shifted with increase in concentration of **6**. Compound **1a** in $CHCl_3$, showed a negative cotton effect around 240 nm. The red-shift in the CD spectral band with increasing concentration of the amphiphiles also suggests stronger interaction among amide groups in the molecular aggregates with increasing concentration. However, the CD spectral profile did not provide any evidence of chiral surface formation. On the other hand, the *N*-palmitoyl or *N*-stearoyl serine amphiphiles formed new chiral surfaces upon self-assembly [29]. This could be due to the presence of longer hydrocarbon tails in these systems, which might provide additional rigidity, particularly, in gel phase to stabilize the chiral surfaces. In the same way, sphingolipids show hydrogen-bonding interaction [18] among amide groups, but the chiral organization has not been observed.

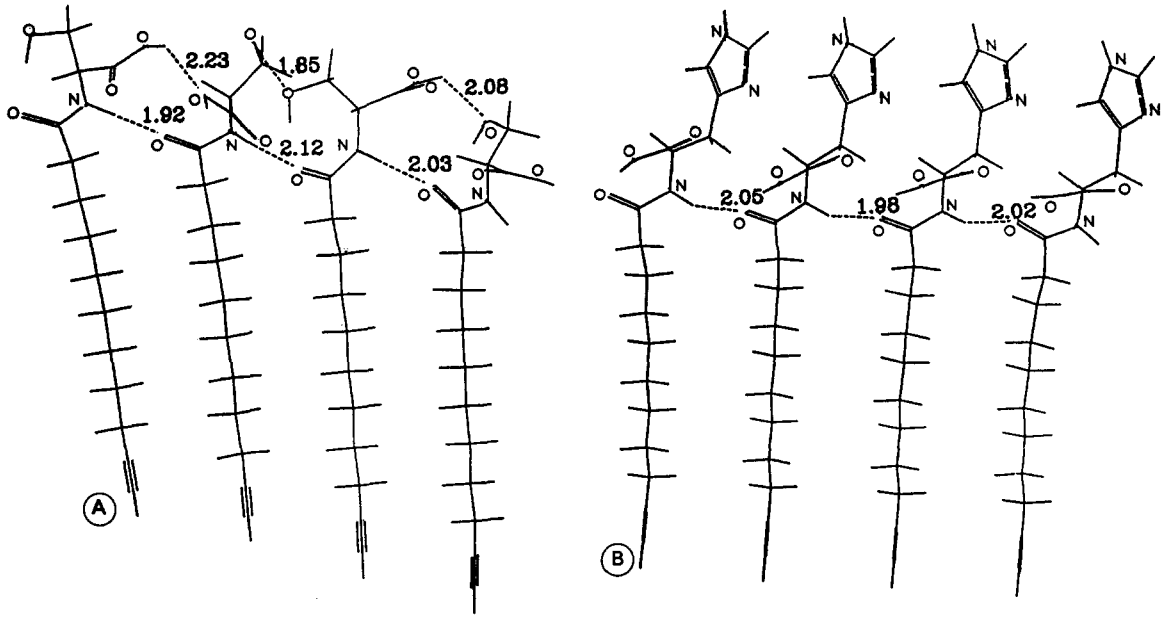

Fig. 3. Model of molecular assembly mode of four adjacent amphiphiles of, (a) **4a**, and (b) **6**. --- = hydrogen-bonding.

4.7. Molecular modelling studies

Molecular modelling studies (Insight II 2.3.0; Biosym Tech., discover force-field, steepest descent algorithm) predict an assembly of the type shown in (Fig. 3a) for the amphiphile **4a**. Two kinds of hydrogen-bonding networks, (a) among amide groups, and (b) among alcoholic groups and the OH groups of the carboxylic acid functions of **4a**, were observed. Similar examination of deprotonated histidine amphiphile assembly shows the existence of intermolecular hydrogen-bonding among amide groups (Fig. 3b) only. This agrees well with the IR, UV-vis and CD results, where intermolecular hydrogen-bonding association among amide groups was predicted. This model indicates an average favoured tilt angle of $\sim 4°$ between neighouring alkyl chains for L-serine amphiphile. [27b].

5. Summary

Self-assembly of chiral amphiphiles involves the association of many weak reversible interactions to obtain a final microstructure that represents the lowest energy form. We believe that two types of strong hydrogen-bonded networks among, (a) the amide groups, and (b) the $-CH_2OH$ and $-CO_2H$ groups (Fig. 3a), presumably, lead to an entangled molecular packing of the serine amphiphile in $CHCl_3$. Indeed, theoretical studies [25] propose that long chiral molecules do not pack parallel to each other, but with a non-zero twist angle with respect to their nearest neighbours. This dense chiral molecular packing leads to molecular tilt [27] and, consequently, results in the twisted form of the molecular assembly into ribbons and tubules. Similar suggestions have also been put forward by Fuhrhop et al. [31] in the case of *N*-alkylaldonamide dispersions. The presence of intertwined and entangled tubules may lead to the fomation of gel [26]. In aqueous medium (pH 7.8), however, the weakened hydrogen-bonding network, coupled with pronounced hydrophobic interactions through the tails, leads to a different kind of supramolecular assembly than that in $CHCl_3$.

In the assembly of histidine amphiphiles, the second type of hydrogen-bonding network may be absent, as observed in the molecular modelling study and this may explain its inability to form the gel.

The tubule formation presumably proceeds from spheres, most probably via helical ribbons

[27]. Thus, 'incorrect' microstructural units get rejected in the dynamic equilibrium assembly and, ultimately, the assemblies with highest stability are produced.

Terminal acetylene moiety, present in the hydrophobic segment of the amphiphile, might be used as a UV marker to study the aggregation since it gives characteristic fine-structure upon aggregation and the presence of 1-ynes do not perturb the nature of the aggregation. The development of nanochemistry is still at primitive stage and much of the contemporary literature is directed toward the strategies for the reproducible synthesis of nanostructures. We are now exploring the effect of introducing additional stabilizing interactions for development of novel microstructure-forming systems. Such studies might provide microstructures with improved kinetic stability.

Acknowledgment

This work was supported by a grant (SP/S1/G32/91) from the Department of Science and Technology, India. We thank the Sophisticated Instruments Facility (SIF) at the Indian Institute of Science for ^{1}H-NMR spectra and electron microscopy and the Supercomputer Education and Research Centre (SERC) for the molecular modelling studies.

References

[1] N. Nakashima, S. Asakuma and T. Kunitake (1985) J. Am. Chem. Soc. 107, 509–511.
[2] K. Yamada, H. Ihara, T. Fukumoto and C. Hirayama (1984) Chem. Lett. 1713–1716.
[3] P. Yager and P. Schoen (1984) Mol. Cryst. Liq. Cryst. 106, 371–381.
[4] M. Markowitz and A. Singh (1991) Langmuir 7, 16–18.
[5] A.S. Rudolph, B.R. Ratna and B. Kahn (1981) Nature 352, 52–54.
[6] D.S. Chung, G.B. Benedek, F.M. Konokoff and J.M. Donovan (1993) Proc. Natl. Acad. Sci. USA. 90, 11341–11345.
[7] D.D. Archibald and S. Mann (1994) Chem. Phys. Lipids 69, 51–64.
[8] D.D. Archibald and P. Yager (1992) Biochemistry 31, 9045–9055.
[9] W. Curatolo and L.J. Neuringer (1986) J. Biol. Chem. 261, 17177–17182.
[10] (a) T. Imae, Y. Takahashi and H. Muramatsu (1992) J. Am. Chem. Soc. 114, 3414–3419; (b) H. Hikada, M. Murata and T. Onai (1984) J. Chem. Soc. Chem. Commun. 562–564.
[11] H. Yanagawa, Y. Ogawa, H. Furuta and K. Tsuno (1989) J. Am. Chem. Soc. 111, 4567–4570.
[12] (a) D.A. Frankel and D.F. O'Brien (1991) J. Am. Chem. Soc. 113, 7436–7437; (b) J-H.Fuhrhop, P. Blumtritt, C. Lehmann and C. Lugar (1991) J. Am. Chem. Soc. 113, 7437–7439.
[13] J-H. Fuhrhop, T. Bedurke, H. Hahn, S. Grund, J. Gatzmann and S. Riederer (1994) Angew. Chem. Int. Ed. Engl. 33, 350–351.
[14] J.C.D. Brand, G. Eglinton and J.F. Morman (1960) J. Chem. Soc. 2526–2533.
[15] J.M. Schnur (1993) Science 262, 1669–1676.
[16] (a) A.K. Lala and E. Ravikumar (1993) J. Am. Chem. Soc. 115, 3982–3988; (b) J. Seelig and A. Seelig (1980) Q. Rev. Biophys. 13,, 19–62.
[17] K. Ogawa, H. Tamura, M. Hatada and T. Ishihara (1988) Langmuir 4, 1229–1233.
[18] D.S. Johnston, S. Sanghera, M. Pons and D. Chapman (1980) Biochim. Biophys. Acta. 602, 57–66.
[19] B.S. Furniss, A.J. Hannaford, V. Rogers, P.W.G. Smith and A.R. Tatchell (1978) in: A.I. Vogel (Ed.), Practical Organic Chemistry, 4th Ed., ELBS, pp. 346.
[20] D.C. Lee, I.R. Miller and D. Chapman (1986) Biochim. Biophys. Acta. 859, 266–270.
[21] Z. Shervani (1993) Colloid. Surfact. A, Physicochem. Eng. Aspects 70, 213–217.
[22] (a) J.H. Fendler (1982) Membrane Mimetic Chemistry, Wiley, New York, pp 37–38; (b) J.-H. Fuhrhop, D. Spiroski and C. Boettcher (1993), J. Am Chem. Soc. 115, 1600–1601.
[23] (a) K. Kalyansundaram (1987) Photochemistry in Microheterogeneous Systems, Academic Press, New York, p. 177; (b) E. Gelade and F.C. De Schryver (1984) in P.L. Luisi and B.E. Straub (Eds.), Reverse Micelles, Plenum Press, New York, pp. 143–164.
[24] (a) G.Santiago, K.N. Houk, G.J. DeCicco and L.T. Scott (1978) J. Am. Chem. Soc. 100, 692–696; (b) E. Kloster-Jensen and J. Wirz (1975) Helv. Chim. Acta 58, 162–177.
[25] R. Neumann and H. Ringsdorf (1986) J. Am. Chem. Soc. 108, 487–490.
[26] Y. Osada and S.B. Ross-Murphy (1993) Sci. Am. 256(5), 42–47.
[27] (a) J.M. Schnur, B.R. Ratna, J.V. Sellinger, A. Singh, G. Jyothi and K.R.K. Easwaran (1994) Science 264, 945–947; (b) W. Helfrich and J. Prost (1993) Phys. Rev. Lett. 71, 4091–4094.
[28] A.S. Rudolph and D.G. Burke (1987) Biochim. Biophys. Acta 902, 349–359.
[29] R.M. Silverstein, G.C. Bassler and T.C. Morril (1991) Spectrometric Identification of Organic Compounds, Wiley, New York, Ch. 3.
[30] (a) M. Shinitzky and R. Haimovitz (1993) J. Am. Chem. Soc. 115, 12545–12549; (b) N.G. Harvey, D. Mirajovsky and E.M. Arnett (1989) J. Am. Chem. Soc. 111, 1115–1122.
[31] J.-H. Fuhrhop, P. Schneider, E. Boekema and W. Helfrich (1988) J. Am. Chem. Soc. 110, 2861–2866.